

**Quantum Chemical DFT and Spectroscopic UV-Vis-NIR Analysis of a series of Push-Pull  
Oligothiophenes End-Capped by Amino/Cyanovinyl Groups**

María Moreno Oliva,<sup>1</sup> Mari Carmen Ruiz Delgado,<sup>1</sup> Juan Casado,<sup>1</sup> M. Manuela M. Raposo,<sup>2</sup> A. Maurício C. Fonseca,<sup>2</sup> Horst Hartmann,<sup>3</sup> Víctor Hernández,<sup>1</sup> and Juan T. López Navarrete.\*<sup>1</sup>

<sup>1</sup> *Department of Physical Chemistry, University of Málaga,  
29071-Málaga, Spain. E-mail: [teodomi@uma.es](mailto:teodomi@uma.es)*

<sup>2</sup> *Centro de Química, Universidade do Minho, Campus de Gualtar,  
4710-057 Braga, Portugal. E-mail: [mfox@quimica.uminho.pt](mailto:mfox@quimica.uminho.pt)*

<sup>3</sup> *Fachbereich Chemie der Fachhochschule Merseburg, Geusaer Strasse,  
D-06217 Merseburg, Germany. E-mail: [Horst.Hartmann@cui.fh-merseburg.de](mailto:Horst.Hartmann@cui.fh-merseburg.de)*

*Abstract:* A series of push-pull chromophores built around thiophene-based  $\pi$ -conjugating spacers and bearing various types of amino-donors and cyanovinyl-acceptors have been analyzed by means of UV-Vis-NIR spectroscopic measurements. Density functional theory (DFT) calculations have also been performed to help the assignment of the most relevant electronic features and to derive useful information about the molecular structure of these NLO-phores. The effects of the donor/acceptor substitution in the electronic and molecular properties of the  $\pi$ -conjugated spacer have been addressed. The effectiveness of the intramolecular charge transfer (ICT) has also been tested as a function of the nature of the end groups (i.e., electron-donating or electron-withdrawing capabilities).

*Keywords:* Spectroscopic properties, push-pull oligomers, electronic structure, nonlinear optics, DFT calculations.

## 1. Introduction

Low band gap polyconjugated organic polymers are quite attractive materials for their applicability in the fabrication of high performance optical and electronic devices [1]. At present, the synthesis of oligomers with well-defined substitution patterns and chain lengths constitutes an alternative way to overcome the problems inherent to the polydispersivity and common insolubility of polymers [2]. The ability of the  $\pi$ -conjugated oligomers as chromophores and electrophores is related to the efficiency of the intramolecular delocalization of  $\pi$ -electrons along the molecular long axis. Thus, one of the main challenges of the research of this class of materials is to investigate the relevant properties of extensively conjugated chains as function of the so-called “effective conjugation length”, qualitatively defined as the length of the molecular domain over which  $\pi$ -delocalization takes place [3].

Electrooptic materials with potential use in photonic devices for telecommunications and optical information processing [4] usually involve a host polymeric matrix containing second-order nonlinear optical (NLO) chromophores either as guest molecules or covalently attached to the polymeric backbone. Dipolar push-pull chromophores constitute the widest class of compounds investigated for their NLO properties [4-10]. These push-pull NLO-phores are basically constituted by an electron-donor (D) and an electron-acceptor (A) group interacting through a  $\pi$ -conjugated spacer.

It is well recognized that the NLO activity of push-pull chromophores is determined not only by the strength of the D-A pair but also more subtly by the  $\pi$ -conjugated spacer [5]. When comparing typical spacers such as polyenes, oligophenylenes or oligothiophenes of the same

chain length and bearing the same D-A pair, a more pronounced redshift (in a given solvent) is commonly observed for the low energy absorption maximum,  $\lambda_{\max}$ , in polyenes than in oligophenylenes or oligothiophenes, indicative of an efficient electron transmission from the donor to the acceptor. The bathochromic shift of the visible absorption of the push-pull chromophore is even more intensified in high polar solvents. This positive solvatochromism has been commonly regarded as an indication of molecular nonlinearity ( $\mu\beta$ ) of NLO-phores [11-13]. However, it was recently reported that some polyenes attached to a strong D-A pair display an inverted solvatochromism [14,15]. Their  $\lambda_{\max}$  exhibit a redshift with an increase of solvent polarity up to a certain polarity limit and then reverse this trend with a further increase of solvent polarity beyond that limit. Clearly, such spectroscopic behavior is not a simple attribute of the D-A strength but it also associated with the electronic properties of the  $\pi$ -conjugated spacer.

Although polyenic systems represents in principle the most effective way to achieve charge redistribution between the donor and the acceptor end groups, and D-A polyenes have been shown to exhibit huge nonlinearities [5], the well-known limited chemical and photothermal stability of extended polyenes might represent an obstacle to the practical applications of the derived NLO-phores. As regards, oligophenylenes, the efficiency of electron transmission is limited by the large aromaticity of the benzene ring, which has a detrimental effect on the second-order polarizabilities. In comparison with oligophenylenes, oligothiophenes behave as very efficient electron relays almost comparable to polyenes [5,16], because of the lower resonance energy of thiophene compared to benzene, and have been shown to give larger contributions to  $\mu\beta(0)$  [12,17,18]. Oligophenylenes attain a rapid saturation beyond the terphenyl unit, whereas oligothiophenes have a strong tendency to increase  $\mu\beta(0)$  with increasing number of thiophene units. Aside from the electron transmission efficiency, another merit of oligothiophenes is their inherent stability from which thiophene-based D-A chromophores

should benefit [19,20].

Some of us have recently reported on the synthesis of several donor-acceptor end-capped oligothiophenes bearing different 5-dialkylamino (D) and 5'-dicyanovinyl or 5'-tricyanovinyl (A) electroactive end groups with the scope of searching new solvatochromic dyes which could act as suited probes for the determination of solvent polarity or as materials with potential applications in NLO (Figure 1) [21]. The longest wavelength optical absorptions of these of thiophene-based push-pull chromophores are polarized along the long molecular axis and strongly influenced by the chemical nature of the electron withdrawing and electron donating end groups. The bathochromic shift and ever-growing intensity with increasing donor and acceptor strength of the end groups is consistent with a charge-transfer (CT) character of this transition. The positive solvatochromic shift of the CT-band of some of these push-pull bithiophenes extends almost over the whole visible range, indicating a large electronic interaction between the two  $\alpha,\alpha'$ -substituents and electron delocalization over the  $\pi$ -conjugated bridge.

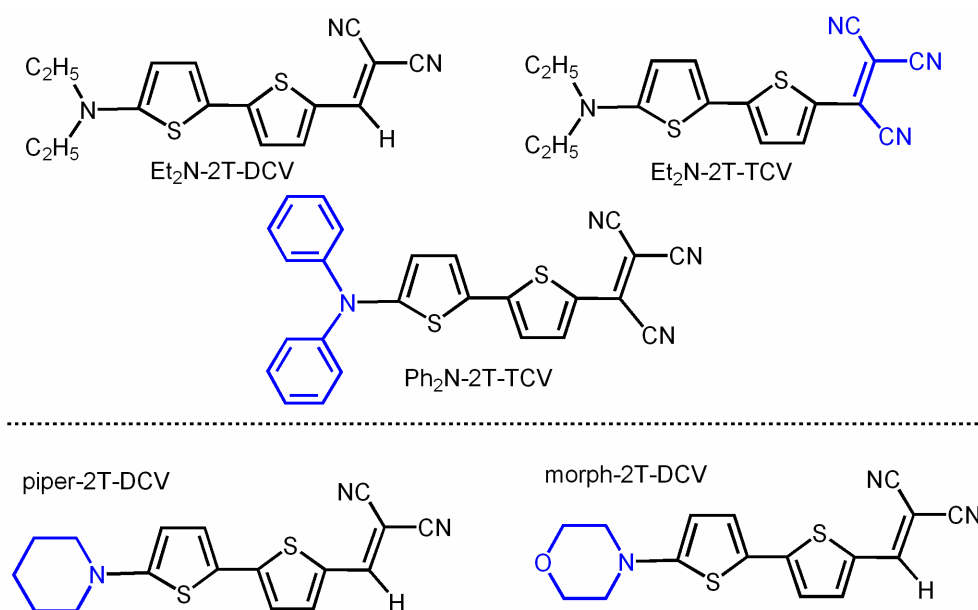


**Figure 1.** Chemical structures and abbreviated notation of the different NLO-phores studied in this study.

Thus, the purpose of this work is to analyze the bunch of push-pull oligothiophenes mentioned above by means of UV-Vis-NIR spectroscopy and DFT calculations with the main aim of deriving information about the interaction between the  $\pi$ -conjugated skeleton and the electroactive end groups. Their photophysical properties and electrochemical activity are also investigated by analyzing the fluorescence emission in solution.

## 2. Experimental and computational details

Figure 1 displays the chemical structures and abbreviated notation of the push-pull oligothiophenes subject of study, which were prepared according to the literature [12c,21b-f].

UV-vis-NIR absorption spectra were recorded at room temperature either on a Lambda 19 Perkin-Elmer dispersive spectrophotometer or on an Agilent 8453 instrument equipped with a diode array for the fast recording of all of the absorptions appearing in the 190-1100 nm spectral region. In the emission experiments, no fluorescent contaminants were detected upon excitation in the wavelength region of experimental interest. Solutions were prepared with an absorbance between 0.1 and 0.2 at the excitation wavelength.

Density Functional Theory (DFT) calculations were carried out by means of the Gaussian 03 program [22] running on SGI Origin 2000 supercomputer. We used the Becke's three-parameter exchange functional combined with the LYP correlation functional (B3LYP) [23]. It has already been shown that the B3LYP functional yields similar geometries for medium-sized molecules as MP2 calculations do with the same basis sets [24,25]. Moreover, the DFT force fields calculated using the B3LYP functional yield infrared spectra in very good agreement with experiments [26,27]. We also made use of the standard 6-31G\*\* basis set [28]. Optimal geometries were determined on isolated entities. All geometrical parameters were allowed to vary independently apart from planarity of the rings.

Vertical electronic excitation energies were computed by using the time-dependent DFT (TDDFT) approach [29,30]. The twenty lowest-energy electronic excited states were at least computed for all the molecules. The computational cost of TDDFT is roughly comparable to that of single-excitation theories based on a HF ground state, such as single-excitation configuration interactions (CIS). Numerical applications reported so far indicate that TDDFT formalism employing current exchange-correlation functionals performs significantly better than HF-based single excitation theories for the low-lying valence excited states of both closed-shell and open-shell molecules [31,32]. TDDFT calculations were carried out using the B3LYP functional and the 6-31G\*\* basis set on the previously optimized molecular geometries obtained at the same level of calculation. Molecular orbital contours were plotted using Molekel 4.3 [33].

### 3. Results and Discussion

#### i) Optimized Geometries

To gain a deeper insight into the changes of the molecular structure induced by the asymmetrical attachment of the D/A groups at the  $\alpha,\omega$ -positions of the  $\pi$ -conjugated backbone, geometry optimizations (DFT//B3LYP/6-31G\*\*) of these push-pull chromophores have been performed. The molecular geometries of all compounds were optimized on the anti arrangement of the thienyl units and without imposing any symmetry constrains. The resulting structures were almost nearly planar, with only a very small twist angle between the two thienyl units, except for the dialkylamino, diarylamino or cyclic amine donor groups. For all the NLO-phores, the amine nitrogen was theoretically predicted to be only slightly pyramidalized (*i.e.*, bearing the N atom a nearly  $sp^2$  hybridation), and with its lone electron pair almost parallel aligned to the  $2p_z$  orbitals of the thienyl carbon atoms, as can be seen in the lateral view of the B3LYP/6-31G\*\* ground-state structure of some compounds plotted in Figure 2.

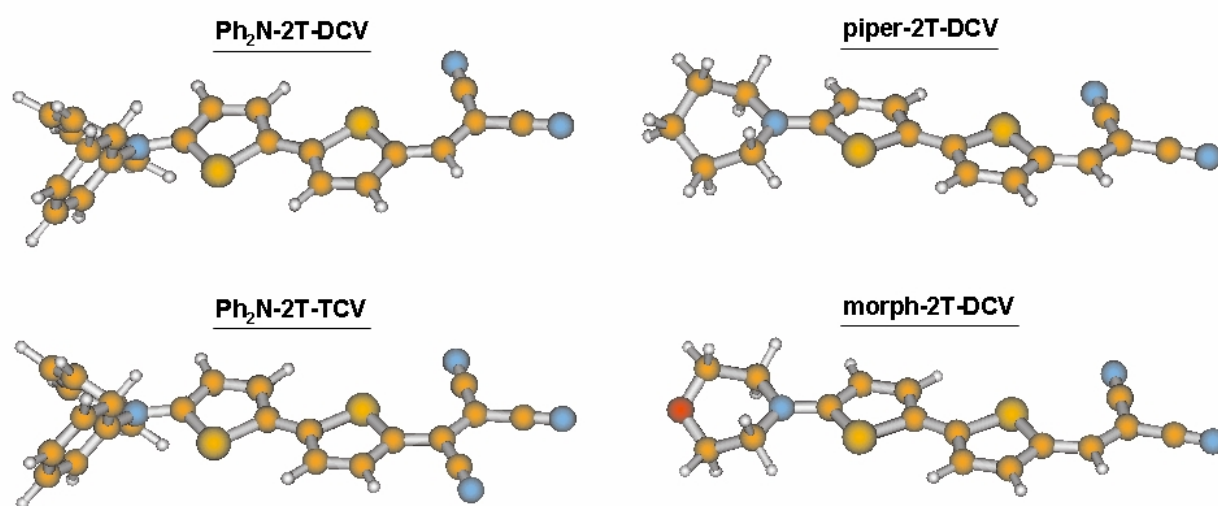


**Figure 2.** Lateral view of the optimized ground-state molecular structures of Ph<sub>2</sub>N-2T-DCV and Ph<sub>2</sub>N-2T-TCV (left), and piper-2T-DCV and morph-2T-DCV (right).

One observes that NLO-phores with a diphenylamine group are more severely twisted

than their corresponding piperidino and morpholino-counterparts due to steric effects between the two pendant phenyl rings and the bithienyl  $\pi$ -core, lowering significantly their  $\pi$ -donor strength. Thus, the outermost phenyl rings are largely distorted (i.e. by  $33^\circ$  for Ph<sub>2</sub>N-2T-DCV and  $25^\circ$  for Ph<sub>2</sub>N-2T-TCV) from the bithiophene moiety, whereas the corresponding angle for morph-2T-DCV is ca.  $10^\circ$ .

To examine in a greater detail the effect of the twist of the amine group on the ground-state polarization of the  $\pi$ -conjugated frame, we optimized the structure of Me<sub>2</sub>N-2T-DCV in four different situations: i) one in which the N lone electron pair was kept in a *syn* conformation with respect to the nearest double bond of the adjacent thiophene ring, ii) the corresponding *anti* conformer, iii) one in which the N atom bears a nearly  $sp^2$  hybridization and iv) one with the N lone pair pointing out of the  $\pi$ -conjugated frame while both N-Me bonds are kept to be tilted out from the bithienyl core least square plane by about  $30^\circ$  (i.e., this models a situation in which the nitrogen should bear a nearly  $sp^3$  hybridization). Due to worse delocalization of the HOMO over the entire NLO-phore in comparison with the non-constrained  $sp^2$ -model structure, one might anticipate higher total energies for the other three spatial orientations of the dialkylamine, as indeed found: thus the anti, syn and  $sp^3$ -model structures were computed to be higher in energy than the minimum-energy  $sp^2$ -one by 6.53, 5.57 and 4.17 Kcal mol<sup>-1</sup>, respectively (i.e., the rotation around the N-C $\alpha$  bond is predicted to be highly hindered in the ground state due to conjugation between the amine donor group and the  $\pi$ -frame). This effective conjugation is also reflected by the significant change of the ground state dipole moment between the various model structures: 8.98 D (anti), 9.49 D (syn), 11.32 D ( $sp^3$ ) and 13.19 D (minimum or near  $sp^2$ ). The topologies and energies of the HOMO frontier orbital for these four models, depicted in Figure 3, illustrate more precisely the large contribution by part of the amine N atom as its lone pair is effectively allowed to freely interact with the  $\pi$ -system of the bithienyl spacer.



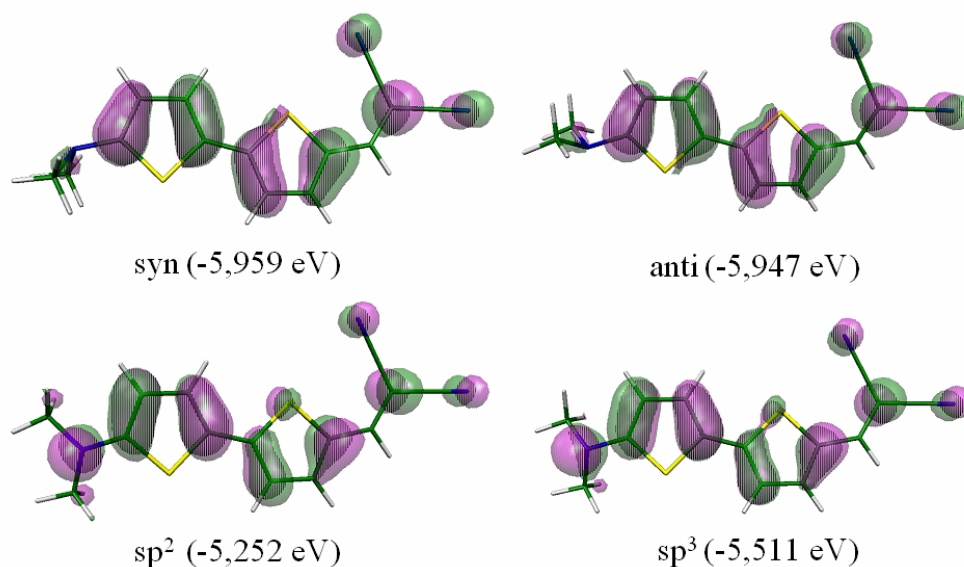


**Figure 3.** Changes in the electronic density contour ( $0.03 e/\text{bohr}^3$ ) and absolute energy for the HOMO orbital of Me<sub>2</sub>N-2T-DCV for the four different spatial orientations of the dimethylamino donor group with respect to the least square plane defined by the bithienyl  $\pi$ -conjugated electron relay.

The atomic orbital compositions of the frontier molecular orbitals for piper-2T-DCV and morph-2T-DCV are sketched in Figure 4. For these two push-pull systems, the corresponding HOMOs and LUMOs display a great resemblance both in topology and energy, what is indicative of the negligible role played by the oxygen atom in the morph-2T-DCV compound.

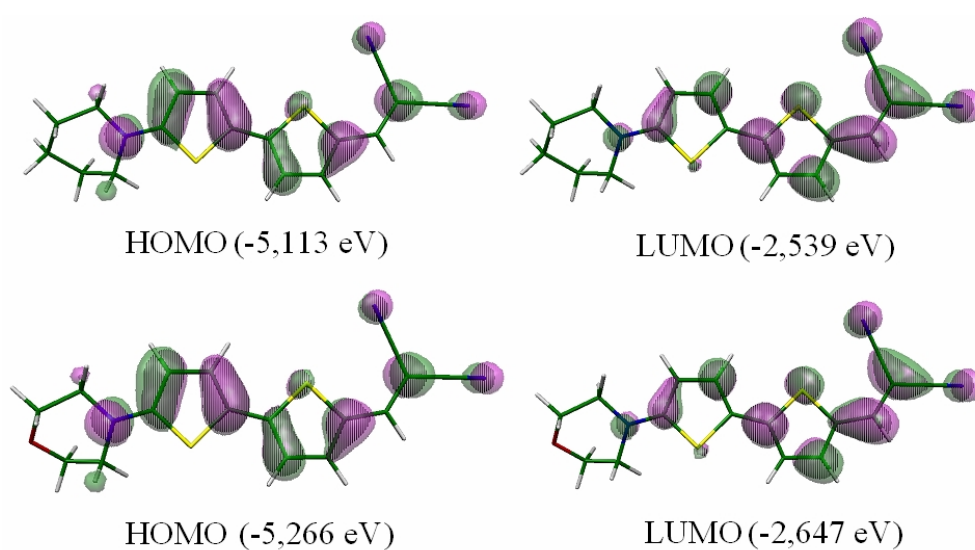


**Figure 4.** Comparison between the electronic density contours ( $0.03 e/\text{bohr}^3$ ) and absolute energies for the HOMOs and LUMOs of piper-2T-DCV (top) and morph-2T-DCV (bottom) .

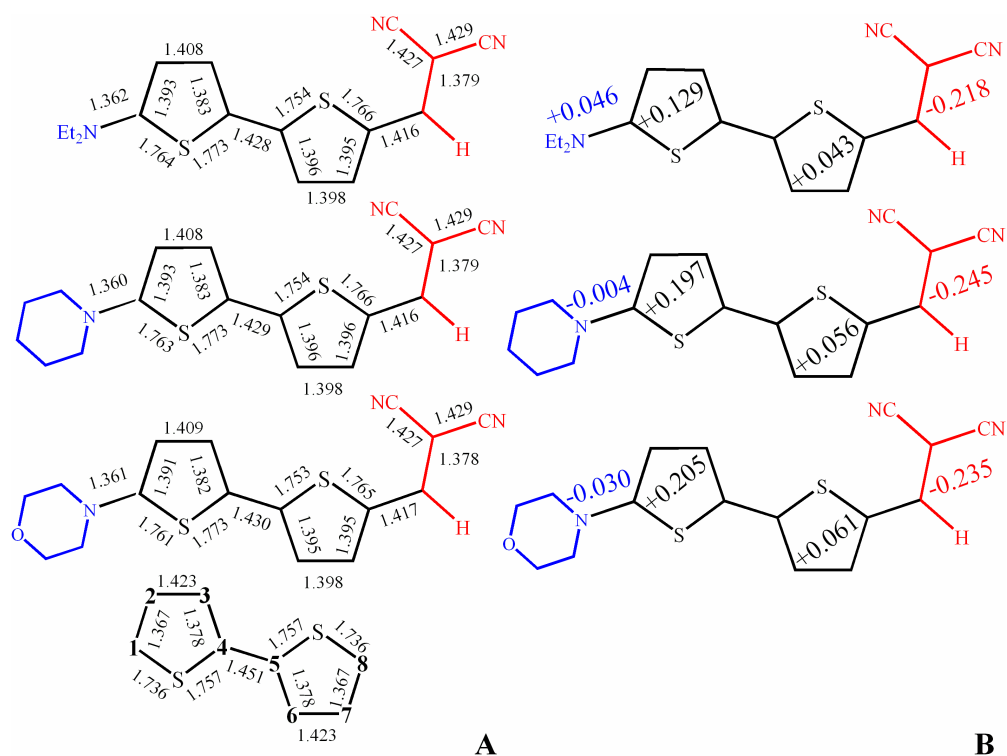


**Figure 5.** DFT//B3LYP/6-31G\*\* optimized structures and overall Mülliken atomic charges on different molecular domains for Et<sub>2</sub>N-2T-DCV, piper-2T-DCV and morph-2T-DCV. The optimized skeletal bond lengths for 2T at the same level of theory are also reported for comparison purposes.

Figure 5 displays a comparison between the optimized B3LYP/6-31G\*\* bond lengths for unsubstituted bithiophene (hereafter referred to as 2T) and for Et<sub>2</sub>N-2T-DCV, piper-2T-DCV and morph-2T-DCV as representative examples of each set of NLO-phores. In addition, it includes the overall Mülliken atomic charges over different molecular domains for the same systems. It can be observed that the attachment of an electron withdrawing DCV group at the end  $\alpha$ -position of the bithienyl electron relay induces the appearance of a strong quinoid character over both thiophene rings (see Figure 5). Thus, for Et<sub>2</sub>N-2T-DCV, the double C<sub>5</sub>=C<sub>6</sub> and C<sub>7</sub>=C<sub>8</sub> (see atom numbering in Figure 5) bonds undergo a lengthening by about 0.018 and 0.028 Å, respectively. Conversely, the skeletal C<sub>1</sub>=C<sub>2</sub> C<sub>2</sub>-C<sub>3</sub> and C<sub>3</sub>=C<sub>4</sub> bond lengths of the thienyl ring linked to the donor change by 0.026, -0.015 and 0.005 Å in the Et<sub>2</sub>N-2T-DCV compound-phore. We want to highlight that the skeletal CC bonds lengths calculated for piper-

2T-DCV and morph-2T-DCV are quite similar to those of Et<sub>2</sub>N-2T-DCV. Finally, the outermost C-S bond lengths are predicted to sizeable increase by near 0.030 Å with respect to 2T. This lengthening however is reflecting three different phenomena: i) the steric interaction between the end-capping groups and the bulky sulfur atoms, ii) the further extension of the  $\pi$ -conjugation from the bithienyl electron-relay towards the donor/acceptor end groups (or in other words, the disappearance upon disubstitution of the end  $\alpha,\alpha'$ -positions of the chain-end effects inherent to 2T, which also justifies for the sizeable lengthening of the C<sub>1</sub>=C<sub>2</sub> and C<sub>7</sub>=C<sub>8</sub> bonds), and iii) the distinct role played by the two S atoms in each NLO-phore.

For Et<sub>2</sub>N-2T-DCV, the difference between the average lengths of the successive skeletal single-double CC bonds (*i.e.*, the *Bond Length Alternation*, BLA, parameter can be regarded as a measure of the degree of quinoidization) of the thienyl rings directly attached to the acceptor and donor amount to 0.003 and 0.020 Å, respectively, while the corresponding value for 2T is 0.051 Å (*i.e.*, the BLA values for the two thienyl rings were computed in each case according to:  $r(C_2C_3) - 0.5 r(C_1C_2) - 0.5 r(C_3C_4)$  or  $r(C_6C_7) - 0.5 r(C_5C_6) - 0.5 r(C_7C_8)$ ). In this regard, we observe that the conjugated C=C/C-C bonds of the bithiophene core are slightly affected by the nature of the donor group (*i.e.*, their computed BLA values are nearly the same).

As shown in Figure 5B, the net charge supported by the acceptor group in Et<sub>2</sub>N-2T-DCV (-0.218 *e*) is much higher than that over the amine donor moiety (+0.046 *e*). Calculations also indicate that the negative charge over the DCV group is mainly balanced by the bithienyl  $\pi$ -conjugated core, which bears positive charges of +0.043 and +0.129 *e* on the thienyl rings linked to the acceptor and donor groups, respectively. Thus, the strong electron withdrawing ability of the cyanovinyl acceptors gives rise to a strong polarization of the  $\pi$ -conjugated backbone, lowering the aromatic character of both thienyl rings.

Finally, if we compare the optimized skeletal C=C/C-C bond lengths of the  $\pi$ -core of Ph<sub>2</sub>N-2T-DCV and Ph<sub>2</sub>N-2T-TCV relative to the corresponding B3LYP/6-31G\*\* values for 2T, a strong quinoid character over the oligothieryl backbone is observed upon the insertion of an additional cyano group in Ph<sub>2</sub>N-2T-TCV (see figure 6). Thus, the attachment of a stronger electron withdrawing group (i.e., TCV) at the end  $\alpha$ -position of the bithienyl moiety increases the degree of polarization of both thiophene rings.

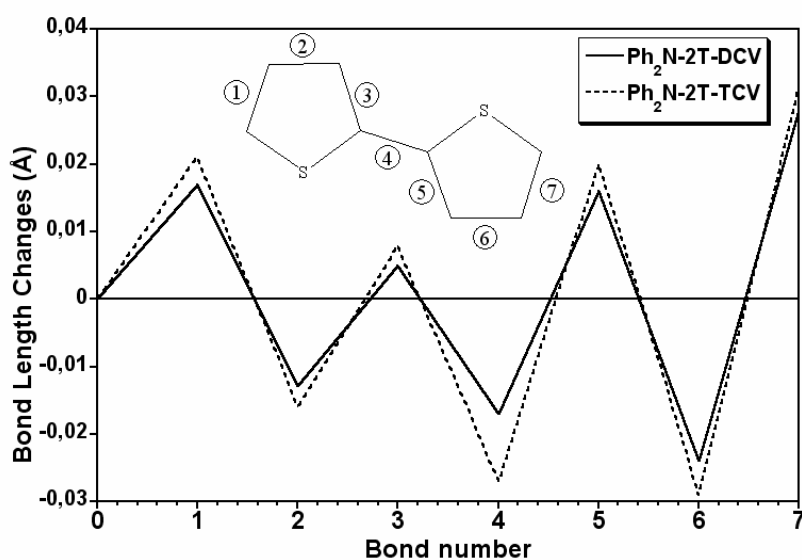


**Figure 6.** Changes of the optimized skeletal C=C/C-C bond lengths of the  $\pi$ -core of Ph<sub>2</sub>N-2T-DCV and Ph<sub>2</sub>N-2T-TCV relative to the corresponding B3LYP/6-31G\*\* values for 2T.

## ii) Optical Properties

### (a) Absorption and emission spectra.

Figure 7 shows the UV-Vis absorption and fluorescence emission spectra of Et<sub>2</sub>N-2T-DCV and piper-2T-DCV in dichloromethane solution. The spectra of 2T are also shown for comparisons purposes.

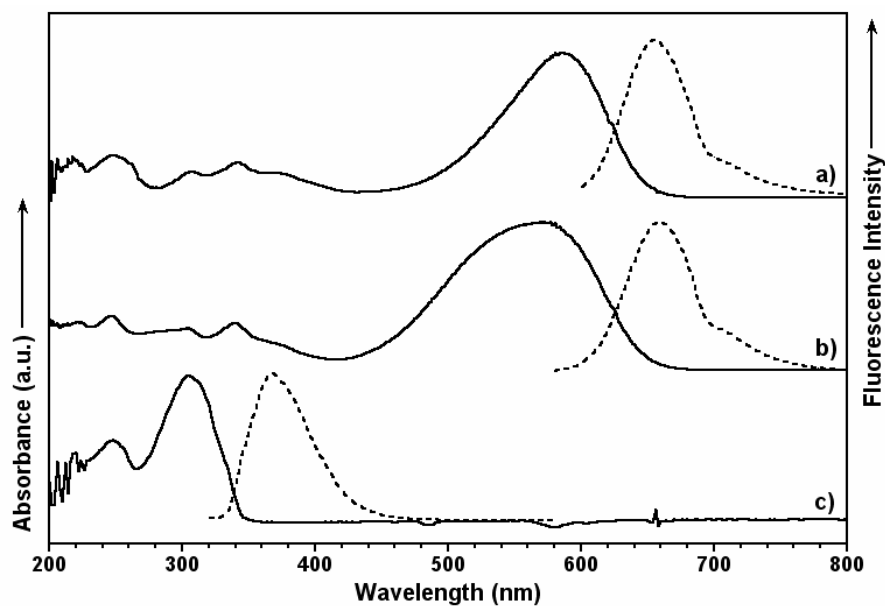


**Figure 7.** UV-Vis absorption (solid line) and fluorescence emission spectra (dotted line) of a) Et<sub>2</sub>N-2T-DCV, b) piper-2T-DCV and d) 2T in CH<sub>2</sub>Cl<sub>2</sub> solution.

The optical spectra of the two D/A systems showed a broad, strong and structure-less visible absorption, with its maximum around 550 nm. The significant redshift of the longest-wavelength absorption by about 200 nm upon donor/DCV substitution of the terminal positions clearly evidences the deeper structural/electronic modifications taking place in the  $\pi$ -conjugated backbones upon push-pull functionalization. On the other hand, there also occurs a redshift of the HOMO-LUMO absorption band on going from piper-2T-DCV (571 nm) to Et<sub>2</sub>N-2T-DCV (585 nm). This redshift of the  $\pi$ - $\pi^*$  absorption to longer wavelengths for the diethylamine NLO-phore might be related with some steric hindrance between the two types of cyclic amines and the nearest thienyl unit, causing a rotation about the C-N bond, and consequently to a less efficient orbital overlapping between the donor-group and the bithienyl electron-relay. Our data are in agreement with those already reported about the strong influence on the thiophene <sup>1</sup>H chemical shift (i.e., H-NMR spectra) of bithiophenes with alkyl (i.e., methyl and ethyl) or heterocyclic amine substituents as the donor units. This effect was attributed to the steric interaction between the thiophene ring and the  $\alpha$ -methylene of the amine which in turn influences

the interaction of the free electron pair on the nitrogen with the  $\pi$ -electron system [34].

Regarding their fluorescence features, nearly the same wavelengths are measured for Et<sub>2</sub>N-2T-DCV (655 nm) and piper-2T-DCV (658 nm), showing similar emission patterns in CH<sub>2</sub>Cl<sub>2</sub> solution. Assuming a charge-transfer emissive state, full planarization of the donor/acceptor end moieties relative to the quinoidized bithienyl electron-relay is presumably expected to occur upon excitation of the  $\pi$ - $\pi^*$  absorption. In such a case, full conjugation between the amine-N atom (i.e., no matter of its surrounding) and the bithienyl-acceptor part of the chromophore likely takes place, thus leading to quite similar fluorescence emission spectra for the whole DCV-set of NLO-phores.

#### **(b) TD-DFT calculations.**

The optical properties of Et<sub>2</sub>N-2T-DCV were investigated theoretically by calculating the lowest-energy electronic excited states using the Time-Dependent TDDFT approach. Experimentally, the UV-Vis spectrum of Et<sub>2</sub>N-2T-DCV exhibits its longest-wavelength absorption at 535 nm (2.32 eV) in non-polar solvents such as cyclohexane. Time-dependent TDDFT calculations in the vacuum predict the occurrence of only one electronic transition in the visible region at 2.56 eV with an oscillator strength ( $f$ ) of 1.00 (i.e., the closest allowed optical transition is predict to appear at 3.63 eV, with  $f = 0.15$ ). The transition at 2.56 eV corresponds to the  $\pi$ - $\pi^*$  excitation to the first singlet excited electronic state and is mainly described by a one-electron promotion from the highest occupied molecular orbital (HOMO) to the lowest unoccupied molecular orbital (LUMO). Although both orbitals spread over the whole molecule, the HOMO displays a larger electron density around the donor group, whereas the LUMO mostly lies on the neighbourhood of the dicyanovinyl group (see Figure 3). Regarding the related Et<sub>2</sub>N-2T-TCV system, the lowest-energy  $\pi$ - $\pi^*$  vertical excitation is predicted by the

single-molecule TDDFT calculations to further redshift to 2.30 eV (with  $f = 0.93$ ), whereas the closest visible absorption should be observed near 3.36 eV, with an oscillator strength of only 0.19. Thus, the strong visible absorption band observed experimentally in each case at the longest wavelength does not have a multiconfigurational character but arises from a single electronic transition, which in its turn implies an electron density transfer from the donor-subunit to the acceptor-subunit. The charge-transfer nature of this optical HOMO  $\rightarrow$  LUMO absorption band is further supported by the enhancement of the dipole moment associated to the electronic transition in the Et<sub>2</sub>N-2T-DCV system, being theoretically calculated to increase from 13.2 D in the ground state to 19.9 D in the first singlet excited state, for the isolated molecule in the vacuum.

In order to evaluate the accuracy of TD-DFT calculations, the experimental oscillator strength,  $f_{\text{expt}}$ , for the optical absorption of Ph<sub>2</sub>-2T-TCV at 685 nm, taken as the prototypical case, was estimated from the conversion between extinction coefficient and oscillator strength,  $f = 4,319 \cdot 10^{-9} (\text{M cm}^2) A$ , where  $A$  is the integrated absorption coefficient. The value of  $A$  is found by determining the area under an absorption band that is displayed as  $x$ -axis = wavenumber ( $\text{cm}^{-1}$ ) against  $y$ -axis = molar absorption coefficient ( $\text{M}^{-1} \text{cm}^{-1}$ ). The units of  $A$  ( $\text{M}^{-1} \text{cm}^{-2}$ ) and the value  $4,319 \cdot 10^{-9} \text{ M cm}^2$  cancel to give the dimensionless value of  $f_{\text{expt}}$ . The accurate estimate of the integrated absorption coefficient for Ph<sub>2</sub>-T<sub>2</sub>-TCV led to  $f_{\text{expt}} \approx 0.602$ , which is in reasonably agreement with the oscillator strength computed for the lowest-lying calculated transition of this chromophore,  $f_{\text{calc}} = 0.893$ ; and what provides another piece of evidence for the quality of the TD-DFT method.

Let us go further in the understanding of the narrowing of the optical gap in those donor/DCV substituted compounds (i.e., taken piper-2T-DCV as a prototypical case) as compared with 2T. Figure 8 displays the MO diagram describing the interaction between DCV-H (dicyanoethane) and the piper-2T fragment. Both the HOMO and LUMO levels are stabilized

in piper-2T-DCV in comparison with those of piper-2T (particularly in the case of the LUMO). Let us now quantitatively account for the main reasons for this behaviour. To this end, it is necessary to consider the energies and topologies of the doubly occupied HOMO and empty LUMO frontier orbitals of the two interacting moieties, the extent of the interaction between their orbitals depends on two main factors: i) the values of the linear combination of atomic orbital (LCAO) coefficients and the symmetry of the MO term (which defines the bonding or antibonding character) of the connecting C atoms, and ii) the relative energy position (energy difference) of the two interacting levels.

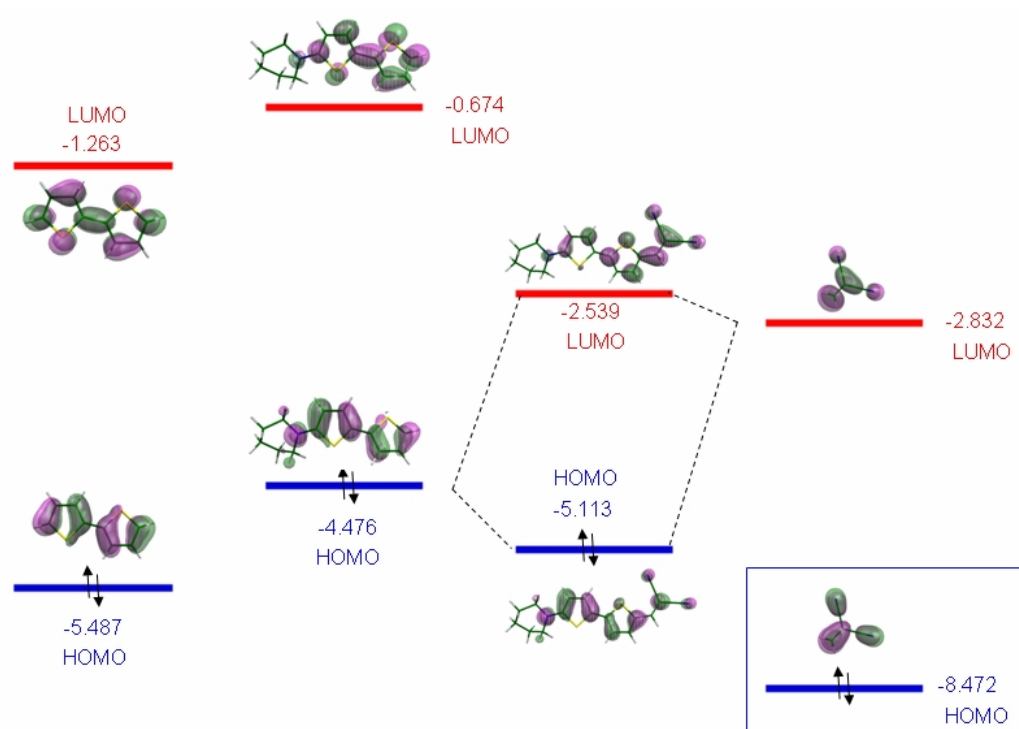


**Figure 8.** B3LYP/6-31G\*\* molecular orbital diagram showing the coupling between the DCV-H and piper-2T fragments of piper-2T-DCV. The HOMO data of DCV-H in blue indicate no mixing with the frontier orbitals of piper-2T. The electronic density contours ( $0.03 e/\text{bohr}^3$ ) and absolute energies of the HOMO (blue) and LUMO (red) orbitals of 2T (left) are also shown for the sake of comparison.

Considering the HOMO of DCV-H, the largest interaction is expected to take place with



doubly occupied  $\pi$  molecular orbitals of piper-2T of similar energies (i.e., near  $-8.5$  eV); hence, the interaction between the DCV-H HOMO and the HOMO of piper-2T is expected to be negligible. The opposite is expected to occur for the interaction between the LUMO of DCV-H and the HOMO of piper-2T, since they are much closer in energy. The coupling between the HOMO of piper-2T and the LUMO of DCV-H thus results in:

- i) A doubly occupied energy level (HOMO of piper-2T-DCV), resulting from their bonding interaction, with a moderate stabilization by  $\approx 0.6$  eV relative to the HOMO of piper-2T).
- ii) An empty molecular orbital due to their antibonding combination, with an energy above the LUMO of DCV-H offset by  $0.3$  eV. The latter orbital becomes the LUMO of the piper-2T-DCV NLO-phore, which in addition is largely stabilized by near  $1.30$  eV with respect to the LUMO of isolated 2T.

Furthermore, this theoretical description reveals that no significant role is played by the 2T LUMO in the LUMO of piper-2T-DCV; at the time that it also highlights to interesting points: i) the HOMO of piper-2T-DCV is mainly accounted for by the bithienyl electron-relay (2T HOMO energy of  $-5.487$  eV and piper-2T-DCV HOMO energy of  $-5.113$  eV), and ii) the LUMO of piper-2T-DCV is mainly accounted for by the dicyanovinyl moiety (DCV-H LUMO energy of  $-2.832$  eV and piper-2T-DCV LUMO energy of  $-2.539$  eV). As another result, from the interaction between the HOMO of piper-2T and the LUMO of DCV-H, a certain piper-2T  $\rightarrow$  DCV electron-density polarization can be anticipated to occur, as a consequence of the partial occupation of the empty orbital of the acceptor at the expense of the doubly occupied HOMO of piper-2T. This fact outlines the sizeable donor-acceptor interaction that accounts for the ground-state electronic structure of these NLO-phores, and which have important consequences on their electrochemical and vibrational properties [35]. Another interesting distinction is that the HOMO  $\rightarrow$  LUMO electronic excitation really corresponds to a virtual displacement of the electron

density from the electron-rich side of the chromophore to the electron-deficient one, that is, a charge-transfer (CT) exciton with seemingly effective electron-hole separation.

#### 4. Conclusions

We have reported on a comprehensive analysis of two sets of push-pull NLO-phores built around a  $\pi$ -conjugated bithienyl electron-relay and bearing various types of amino-donor groups and either a dicyanovinyl (DCV) or tricyanovinyl (TCV) moiety as the acceptor.

The molecular geometry optimizations reveal a substantial degree of quinoidization of the  $\pi$ -conjugated backbone of both sets of NLO-phores, with a full reversal of the geometry of the thienyl ring linked to the DCV acceptor group from an aromatic-like pattern to a quinoid-like one. Furthermore, the B3LYP/6-31G\*\* Mülliken atomic charge distribution also indicates that the net charge over the acceptor moiety is substantially higher than the overall charge on the amine-donor group, and that the  $\pi$ -conjugated electron relay is strongly polarized since it bears nearly the 70% of the net positive charge of the zwitterionic form of the NLO-phore.

All the D- $\pi$ -A systems studied in this paper showed an intramolecular charge transfer band in their visible absorption spectra, whose position is influenced both by the nature of the end groups. The topologies and energies of the molecular orbitals were studied by means of TDDFT//B3LYP/6-31G\*\* showing that the HOMO-LUMO energy gaps account for the observed intramolecular charge transfer from the donor-subunit to the acceptor-subunit.

Finally, density functional theory has been shown to provide support for the observed electronic and optical properties of the systems studied in this work, offering excellent correlations with the measured quantities. The power and usefulness of both DFT and TDDFT model chemistry calculations have been thus well documented. The present study offers opportunity for further development of novel functional organic materials for electronic applications in addition of providing a basic understanding of the mechanisms governing the

electron-transfer processes in  $\pi$ -conjugated donor-acceptor arrays.

### Acknowledgment

Research at the University of Málaga was supported by the Ministerio de Educación y Ciencia (MEC) of Spain through project CTQ2006-14987-C02-01, and by the Junta de Andalucía for funding our FQM-0159 scientific group. J.C. is grateful to the Ministerio de Ciencia y Tecnología of Spain for a Ramón y Cajal position of Chemistry at the University of Málaga. M.C.R.D. is also grateful to the Ministerio de Educación y Ciencia of Spain for a personal grant. The group at the University of Minho acknowledges the Foundation for Science and Technology (Portugal) for financial support through Centro de Química (UM) and through POCTI, FEDER (ref. POCTI/QUI/37816/2001). M. Manuela M. Raposo and A. Maurício C. Fonseca are also grateful to Professor G. Kirsch from University of Metz (France) for his collaboration.

### References

- [1] (a) T.A. Skotheim, R.L. Elsenbaumer, J.R. Reynolds, *Handbook of Conducting Polymers*, 2nd ed, Eds: Marcel Dekker, New York (1998). (b) W.R. Salaneck, I. Lundstrom, B. Ranby, *Conjugated Polymers and Related Materials*, Eds: Oxford University Press, Oxford, U.K. (1993).
- [2] (a) K. Müllen, G. Wegner, *Electronic Materials: The Oligomeric Approach*, Eds: Wiley-VCH, Weinheim, Germany (1998). (b) D. Fichou, *Handbook of Oligo and Polythiophenes*, Eds: Wiley-VCH, New York (1999).
- [3] (a) H.-H. Hörold, W. Helbig, *Macromol. Chem., Macro. Symp.* **12** 229 (1987). (b) H.-H. Hörold, J. Offermann, P. Atrat, K.D. Tauer, G. Drefahl, *Tr. Mezhdunar. Symp.* 171 (1975), *Chem. Abstr.* **85** 124388.

- [4] (a) P.N. Prasad, D.J. Williams, *Introduction to Nonlinear Optical Effects in Molecules and Polymers*, Wiley: New York (1991). (b) J. Zyss, *Molecular Nonlinear Optics: Materials, Physics and Devices*, Academic Press: Boston (1993). (c) D.R. Kanis, M.A. Ratner, T.J. Marks, *Chem. Rev.* **94** 195 (1994). (d) S.R. Marder, J.W. Perry, *Adv. Mater.* **5** 804 (1993). (e) T.J. Marks, M.A. Ratner, *Angew. Chem. Int. Ed. Engl.* **34** 155 (1995). (f) L.R. Dalton, A.W. Harper, R. Ghosn, W.H. Steier, M. Ziari, H. Fetterman, Y. Shi, R.V. Mustacich, A.K.-Y. Jen, K.J. Shea, *Chem. Mater.* **7** 1060 (1995). (g) Y. Shi, C. Zhang, J.H. Bechtel, L.R. Dalton, B.H. Robinson, W.H. Steier, *Science* **288** 119 (2000). (h) J. Wolf, R. Wortmann, *Adv. Phys. Org. Chem.* **32** 121 (1999). (i) N.J. Long, *Angew. Chem. Int. Ed. Engl.* **34** 21 (1995). (j) A.R. Brown, A. Pomp, C.M. Hart, D.M. de Leeuw, *Science* **270** 972 (1995). (k) R.H. Friend, R.W. Gymer, A.B. Holmes, J.H. Burroughes, R.N. Marks, C. Taliani, D.D.C. Bradley, D.A. Dos Santos, J.-L. Brédas, M. Lögdlund, W.R. Salaneck, *Nature* **397** 121 (1999).
- [5] (a) S.R. Marder, C.B. Gorman, B.G. Tiemann, L.T. Cheng, *J. Am. Chem. Soc.* **115** 3006 (1993). (b) S.R. Marder, L.T. Cheng, B.G. Tiemann, *J. Chem. Soc., Chem. Commun.* 672 (1992). (c) S.R. Marder, L.T. Cheng, B.G. Tiemann, A.C. Friedli, M. Blanchard-Desce, J.W. Perry, J. Skindhoj, *Science* **263** 511 (1994).
- [6] (a) G. Mignani, F. Leising, R. Meyreux, H. Samson, *Tetrahedron Lett.* **31** 4743 (1990). (b) A.K.-Y. Jen, V.P. Rao, K.J. Drost, K.Y. Wong, M.P. Cava, *J. Chem. Soc., Chem. Commun.* 2057 (1994). (c) V.P. Rao, Y.M. Cai, A.K.-Y. Jen, *J. Chem. Soc., Chem. Commun.* 1689 (1994).
- [7] V.P. Rao, A.K.-Y. Jen, K.Y. Wong, K.J. Drost, *J. Chem. Soc., Chem. Commun.* 1118 (1993). (b) S. Gilmour, R.A. Montgomery, S.R. Marder, L.-T. Cheng, A.K.-Y. Jen, Y. Cai, J.W. Perry, L.R. Dalton, *Chem. Mater.* **6** 1603 (1994). (c) P. Boldt, G. Bourhill, C. Bräuchle, Y. Jim, R. Kammler, C. Müller, J. Rase, J. Wichern, *Chem. Commun.*, 793

- (1996). (d) X. Wu, J. Wu, Y. Liu, A.K.-Y. Jen, *J. Am. Chem. Soc.* **121** 472 (1999). (e) X. Wu, J. Wu, Y. Liu, A.K.-Y. Jen, *Chem. Commun.* 2391 (1999).
- [8] (a) S.-S. Sun, C. Zhang, L.R. Dalton, S.M. Garner, A. Chen, W.H. Steier, *Chem. Mater.* **8** 2539 (1996). (b) A.K.-Y. Jen, Y. Liu, L. Zheng, S. Liu, K.J. Drost, Y. Zhang, L.R. Dalton, *Adv. Mater.* **11** 452 (1999).
- [9] (a) V.P. Rao, A.K.-Y. Jen, K.Y. Wong, K.J. Drost, *Tetrahedron Lett.* **34** 1747 (1993). (b) V.P. Rao, C. Cai, I. Liakatas, M.-S. Wong, M. Bösch, C. Bosshard, P. Günter, S. Concilio, N. Tirelli, U.W. Suter, *Org. Lett.* **1** 1847 (1999).
- [10] (a) S.R. Marder, J.W. Perry, G. Bourhill, C.B. Gorman, B.G. Tiemann, K. Mansour, *Science* **261** 186 (1993). (b) S.R. Marder, C.B. Gorman, F. Meyers, J.W. Perry, G. Bourhill, J.-L. Brédas, B.M. Pierce, *Science* **265** 632 (1994).
- [11] (a) M. Barzoukas, M. Blanchard-Desce, D. Josse, J.-M. Lehn, J. Zyss, *Chem. Phys.* **133** 323 (1989). (b) A. Slama-Schowk, M. Blanchard-Desce, J.-M. Lehn, *J. Phys. Chem.* **94** 3894 (1990). (c) M. Blanchard-Desce, R. Wortmann, S. Lebus, J.-M. Lehn, P. Krämer, *Chem. Phys. Lett.* **243** 526 (1995). (d) M. Blanchard-Desce, C. Runser, A. Fort, M. Barzoukas, J.-M. Lehn, V. Bloy, V. Alain, *Chem. Phys.*, **199** 253 (1995). (e) T. Verbiest, S. Houbrechts, M. Kauranen, K. Clays, A. Peersons, *J. Mater. Chem.* **7** 215 (1997). (f) O.-K. Kim, A. Fort, M. Barzoukas, M. Blanchard-Desce, J.-M. Lehn, *J. Mater. Chem.* **9** 2227 (1999).
- [12] (a) F. Effenberger, F. Würthner, *Angew. Chem. Int. Ed. Engl.* **32** 712 (1993). (b) F. Würthner, F. Effenberger, R. Wortmann, P. Krämer, *Chem. Phys.* **173** 305 (1993). (c) F. Effenberger, F. Würthner, F. Steybe, *J. Org. Chem.* **60** 2082 (1995). (d) F. Steybe, F. Effenberger, U. Gubler, C. Bosshard, P. Günter, *Tetrahedron* **54** 8469 (1998).
- [13] I. Cabrera, O. Althoff, H.-T. Man, H.N. Yoon, *Adv. Mater.* **6** 43 (1994).

- [14] S.R. Marder, J.W. Perry, B.G. Tiemann, C.B. Gorman, S. Gilmour, S.L. Biddle, G. Bourhill, *J. Am. Chem. Soc.* **115** 2524 (1993).
- [15] M. Blanchard-Desce, V. Alain, P.V. Bedworth, S.R. Marder, A. Fort, C. Runser, M. Barzoukas, S. Lebus, R. Wortmann, *Chem. Eur. J.* **3** 1091 (1997).
- [16] (a) V.P. Rao, A.K.-Y. Jen, Y. Cai, *J. Chem. Soc., Chem. Commun.* 1237 (1996). (b) A.K.-Y. Jen, Y. Cai, P.V. Bedworth, S.R. Marder, *Adv. Mater.* **9** 132 (1997).
- [17] L.-T. Cheng, W. Tam, S.R. Marder, A.E. Stiegman, G. Rikken, C.W. Spangler, *J. Phys. Chem.* **95** 10643 (1991).
- [18] I. Ledoux, J. Zyss, A. Jutand, C. Amatore, *Chem. Phys.* **150** 117 (1991).
- [19] S. Gilmore, S.R. Marder, J.W. Perry, L.-T. Cheng, *Adv. Mater.* **6** 494 (1994).
- [20] V.P. Rao, K.Y. Wong, A.K.-J. Jen, K.J. Drost, *Chem. Mater.* **6** 2210 (1994).
- [21] (a) L.G.S. Brooker, G.H. Keyes, D.W. Heseltine, *J. Am. Chem. Soc.* **73** 5350 (1951). (b) K. Eckert, A. Schröder, H. Hartmann, *Eur. J. Org. Chem.* 1327 (2000). (c) H. Hartmann, K. Eckert, A. Schröder, *Angew. Chem. Int. Ed.* **39** 556 (2000). (d) M.M.M. Raposo, G. Kirsch, *Tetrahedron.* **59** 4891 (2003). (e) M.M.M. Raposo, M.C. Fonseca, G. Kirsch, *Tetrahedron.* **60** 4071 (2004). (f) P.V. Bedworth, Y. Cai, A. Jen, S.R. Marder, *J. Org. Chem.* **61** 2242 (1996).
- [22] M.J. Frisch, G.W. Trucks, H.B. Schlegel, G.E. Scuseria, M.A. Robb, J.R. Cheeseman, J.A.Jr. Montgomery, T. Vreven, K.N. Kudin, J.C. Burant, J.M. Millam, S.S. Iyengar, J. Tomasi, V. Barone, B. Mennucci, M. Cossi, G. Scalmani, N. Rega, G.A. Petersson, H. Nakatsuji, M. Hada, M. Ehara, K. Toyota, R. Fukuda, J. Hasegawa, M. Ishida, T. Nakajima, Y. Honda, O. Kitao, H. Nakai, M. Klene, X. Li, J.E. Knox, H.P. Hratchian, J.B. Cross, C. Adamo, J. Jaramillo, R. Gomperts, R.E. Stratmann, O. Yazyev, A.J. Austin, R. Cammi, C. Pomelli, J.W. Ochterski, P.Y. Ayala, K. Morokuma, G.A. Voth, P. Salvador, J.J. Dannenberg, V.G. Zakrzewski, S. Dapprich, A.D. Daniels, M.C. Strain,

- O. Farkas, D.K. Malick, A.D. Rabuck, K. Raghavachari, J.B. Foresman, J.V. Ortiz, Q. Cui, A.G. Baboul, S. Clifford, J. Cioslowski, B.B. Stefanov, G. Liu, A. Liashenko, P. Piskorz, I. Komaromi, R.L. Martin, D.J. Fox, T. Keith, M.A. Al-Laham, C.Y. Peng, A. Nanayakkara, M. Challacombe, P.M.W. Gill, B. Johnson, W. Chen, M.W. Wong, C. Gonzalez, J.A. Pople, *Gaussian 03, Revision B.04*; Gaussian Inc.: Pittsburgh PA (2003).
- [23] A.D. Becke, *J. Chem. Phys.* **98** 1372 (1993).
- [24] P.J. Stephens, F.J. Devlin, F.C.F. Chabalowski, M.J. Frisch, *J. Phys. Chem.* **98** 11623 (1994).
- [25] J.J. Novoa, C. Sosa, *J. Phys. Chem.* **99** 15837 (1995).
- [26] A.P. Scott, L. Radom, *J. Phys. Chem.* **100** 16502 (1996).
- [27] G. Rauhut, P. Pulay, *J. Phys. Chem.* **99** 3093 (1995).
- [28] M.M. Francl, W.J. Pietro, W.J. Hehre, J.S. Binkley, M.S. Gordon, D.J. Defrees, J.A. Pople, *J. Chem. Phys.* **77** 3654 (1982).
- [29] E. Runge, E.K.U. Gross, *Phys.Rev.Lett.* **52** 997 (1984). E.K.U. Gross, W. Kohn, *Adv.Quantum Chem* **21** 255 (1990). E.K.U. Gross, R.M. Driezler, Eds: Plenum Press, New York 149 (1995).
- [30] M.E. Casida, *Recent Advances in Density Functional Methods, Part I*, D.P. Chong, Eds: World Scientific, Singapore, 115 (1995).
- [31] W. Koch, M.C. Holthausen, *A Chemist's Guide to Density Functional Theory*, Wiley-VCH, Weinheim (2000).
- [32] J. Casado, L.L. Miller, K.R. Mann, T.M. Pappenfus, Y. Kanemitsu, E. Ortí, P.M. Viruela, R. Pou-Amérigo, V. Hernández, J.T. López Navarrete, *J. Phys. Chem. B* **106** 3872 (2002).
- [33] S. Portmann, H.P. Lüthi, *Chimia* **54** 766 (2000).
- [34] R. Radeaglia, H. Hartmann, S. Scheithauer, *Z. Naturforsch.* **24B** 286 (1969).

- [35] M. Moreno Oliva, J. Casado, M.M.M. Raposo, A.M.C. Fonseca, H. Hartmann, V. Hernández, J.T. López Navarrete, *J. Org. Chem.* **71** 7509 (2006).